Nanoscale Research Letters
a SpringerOpen Journal

NANO EXPRESS Open Access

# Ferromagnetism in exfoliated tungsten disulfide nanosheets

Xingze Mao[1], Yan Xu[2], Qixin Xue[1], Weixiao Wang[1] and Daqiang Gao[1*]

**Abstract**

Two-dimensional-layered transition metal dichalcogenides nanosheets have attracted tremendous attention for their promising applications in spintronics because the atomic-thick nanosheets can not only enhance the intrinsic properties of their bulk counterparts, but also give birth to new promising properties. In this paper, ultrathin tungsten disulfide ($WS_2$) nanosheets were gotten by liquid exfoliation route from its bulk form using dimethylformamide (DMF). Compared to the antiferromagnetism bulk $WS_2$, ultrathin $WS_2$ nanosheets show intrinsic room-temperature ferromagnetism (FM) with the maximized saturation magnetization of 0.004 emu/g at 10 K, where the appearance of FM in the nanosheets is partly due to the presence of zigzag edges in the magnetic ground state at the grain boundaries.

**Keywords:** WS2, ferromagnetism, nanosheet

## Background

Together with the rapidly increasing research interests on graphene and their devices in the last few years, inorganic-layered structure materials, such as tungsten disulfide ($WS_2$) and $MoS_2$ also attracted extensive attention because of their unique physics properties [1-5]. Similar to graphite, such layered structure materials crystallize in a van der Waals-layered structure where each layer consists of a slab of S-X-S ($X$ = W, Mo) sandwich. $MoS_2$ monolayers have been isolated via mechanical exfoliation, wet chemical approaches, physical vapor deposition, and sulfurization of molybdenum films [6-9]. At the same time, their electronic, optical, and magnetic properties including carrier mobilities of approximately 200 $cm^2V^{-1}s^{-1}$, photoluminescence, and weak room temperature ferromagnetism have been proposed [1-5,10,11]. So far, $MoS_2$ has been explored in diverse fields and integrated in transistors and sensors, and used as a solid-state lubricant and catalyst for hydrodesulfurization, hydrogen evolution, and so on [6-9,12,13].

Recently, mechanically exfoliated, atomically thin sheets of $WS_2$ were also shown to exhibit high in-plane carrier mobility and electrostatic modulation of conductance similar to $MoS_2$ [14,15]. Differential reflectance and photoluminescence spectra of mechanically exfoliated sheets of synthetic 2H-$WS_2$ with thicknesses ranging between 1 and 5 layers were also reported, where the excitonic absorption and emission bands were found as gradually blue shifted with decreasing number of layers due to geometrical confinement of excitons [16]. Gutiérrez et al. described the direct synthesis of $WS_2$ monolayers via sulfurization of ultrathin $WO_3$ films with triangular morphologies and strong room-temperature photoluminescence [17], which could be used in applications including the fabrication of flexible/transparent/low-energy optoelectronic devices.

Even though the electrical, mechanical, and optical properties of $WS_2$ have been studied both theoretically and experimentally, recent studies on the magnetic response of $WS_2$ are limited. Murugan et al. revealed by first-principles calculations that stoichiometric $Mo_nS_{2n}$ ($n$ = 1, 2, 5, and 6) and $W_6S_{12}$ clusters as well as several of the nonstoichiometric clusters are magnetic, where the magnetic moments arise due to the partially filled $d$ states [18]. Besides, calculation results indicate that adsorption of nonmetal elements on the surface of $WS_2$ nanosheets can induce a local magnetic moment [19]. In an experimental study, Matte et al. fabricated $WS_2$ nanosheets by hydrothermal method and revealed their

* Correspondence: gaodq@lzu.edu.cn
[1]Key Laboratory for Magnetism and Magnetic Materials of MOE, Lanzhou University, Lanzhou 730000, People's Republic of China
Full list of author information is available at the end of the article

ferromagnetism, which was considered to be related to the edges and defects [20].

Developed liquid exfoliation process is considered to be an effective pathway to prepare the ultrathin two-dimensional nanosheets of intrinsically layered structural materials with high quality [21]. In this paper, the ultrathin $WS_2$ nanosheets were gotten by exfoliating bulk $WS_2$ in *N*,*N*-dimethylformamide (DMF, 100 mL) solution as in our previous report [22], and we studied the magnetic properties of $WS_2$ nanosheets experimentally from 300 K down to 10 K. Results indicate that the fabricated $WS_2$ nanosheets show clear room-temperature ferromagnetism which possibly originates from the existence of zigzag edges or defects with associated magnetism at grain boundaries.

## Methods

$WS_2$ nanosheets were prepared through exfoliating of bulk $WS_2$. In a typical synthesis progress, 0.5 g of $WS_2$ powders was sonicated in N, N-Dimethylformamide (DMF, 100 mL) to disperse the powder. After precipitation, the black dispersion was centrifuged at 2000 rpm for about 20 minutes to remove the residual large-size $WS_2$ powders. Then, the remainder solution was centrifuged at 10000 rpm for 1 h to obtain the black products. To remove the excess surfactant, the samples were repeatedly washed with ethanol and centrifuged. Finally, the samples were dried at 60°C in vacuum condition.

## Results and discussion

Figure 1a shows the schematic illustration of liquid exfoliation process from bulk $WS_2$ to ultrathin nanosheets. When ultrasonication was carried out in the DMF solution, the $WS_2$ bulk materials swelled with the insertion of DMF molecules into the layers, which can then be easily exfoliated into the nearly transparent ultrathin nanosheets. In the absence of any high-temperature treatment or oxidation process, the exfoliated nanosheets will retain the same crystal structure of the bulk materials. Typical X-ray diffraction (XRD, X' Pert PRO Philips with Cu Kα radiation; Philips, Anting, Shanghai, China) patterns of the $WS_2$ bulk and nanosheets are reported in Figure 1b. During the XRD test, the exfoliated $WS_2$ nanosheets were collected together onto the glass substrate. That is to say, the XRD result can be gotten just as the other powder sample in

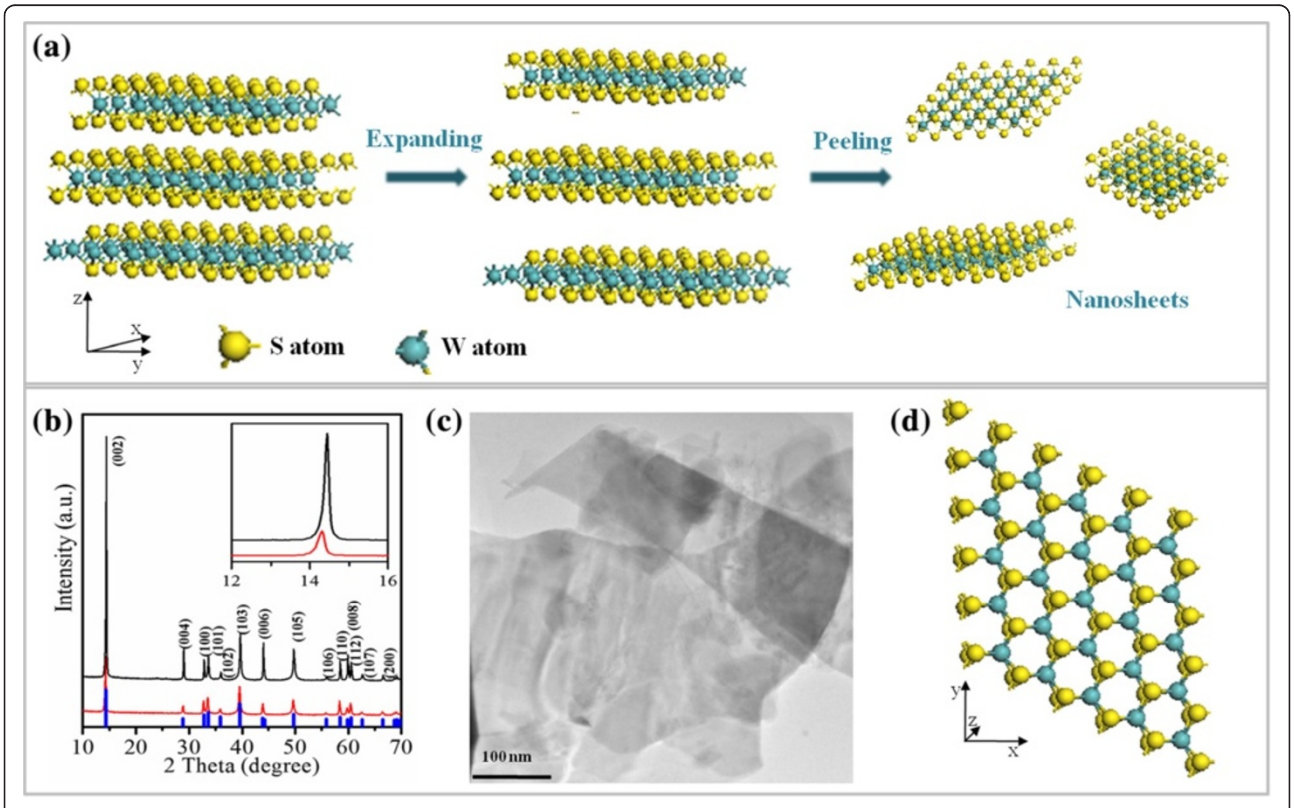


**Figure 1 Schematic illustration of liquid exfoliation process, XRD results, TEM, and theoretically perfect crystal structure of $WS_2$. (a)** Schematic illustration of liquid exfoliation process from bulk $WS_2$ to ultrathin nanosheets. **(b)** XRD results for pristine $WS_2$ bulk (black line) and the exfoliated nanosheets (red line), the blue line is the standard $WS_2$ diffraction peaks got from JCPDS card no. 85-1068. **(c)** TEM image of the exfoliated $WS_2$ nanosheets. **(d)** A theoretically perfect crystal structure of the single-layered $WS_2$.

our case. It can be seen that all the diffractions for the exfoliated nanosheets are corresponding to the hexagonal phase of $WS_2$ (JCPDS card no. 85-1068) and as comparable to the bulk form. The dominated (002) diffraction peak indicates the growth of $WS_2$ along the *c*-axis direction. Results indicate that the (002) peak for the exfoliation nanosheets decreased in intensities when compared to the pristine $WS_2$, and the notable shift to the low intensity was also observed, which may be caused by the decrease of structural crystalline and the increasing of the disorder or defect density [23]. Figure 1c shows the transmission electron microscopy (TEM, TecnaiTM G2 F30, FEI, Hillsboro, OR, USA) image of the exfoliated product, from which one can see that the free-standing nanosheets were inhomogenous with different sizes and morphologies.

High-resolution TEM (HRTEM) image and the two-dimensional fast Fourier transform (FFT) analysis (Figure 2b,c) reveal the hexagonal lattice structure with the lattice spacing of 0.27 and 0.16 nm assigned to the (100) and (110) planes [17]. Further high-resolution TEM results for the selected regions for the inner and the edges of one nanosheet are shown in Figure 2b,d, respectively. Results indicate that the inner part of the nanosheets has a well-crystallographic structure without existence of defects. On the contrary, a clear disorder is observed at the edges; the result reveals a hexagonal arrangement of atoms with zigzag edges. The size distribution of as-prepared $WS_2$ nanosheets was evaluated from the tapping-mode atomic force microscopy (AFM Dimension 3100 with Nanoscope IIIa controller, Veeco, CA, USA). As can be seen from Figure 2e, the diameter of the nanosheets ranges from 200 to 500 nm, in accordance with the TEM observation. As also shown in Figure 2e, the randomly measured thicknesses for the nanosheets are ranging from 1.2 to 4.8 nm, where the maximum height profile of 4.9 nm is shown in Figure 2g. Considering that the *c* parameter of $WS_2$ is 0.62 Å, the thickness of 1.8 to 4.9 nm denoted that the nanosheets comprised 2 ~ 8 single layers of $WS_2$. Accidentally, some $WS_2$ nanosheets have curled edges, rendering it possible to evaluate a sheet thickness during high-resolution TEM. One can see from Figure 2f that the nanosheet with 3 ~ 8 layers thick shows the presence of a high

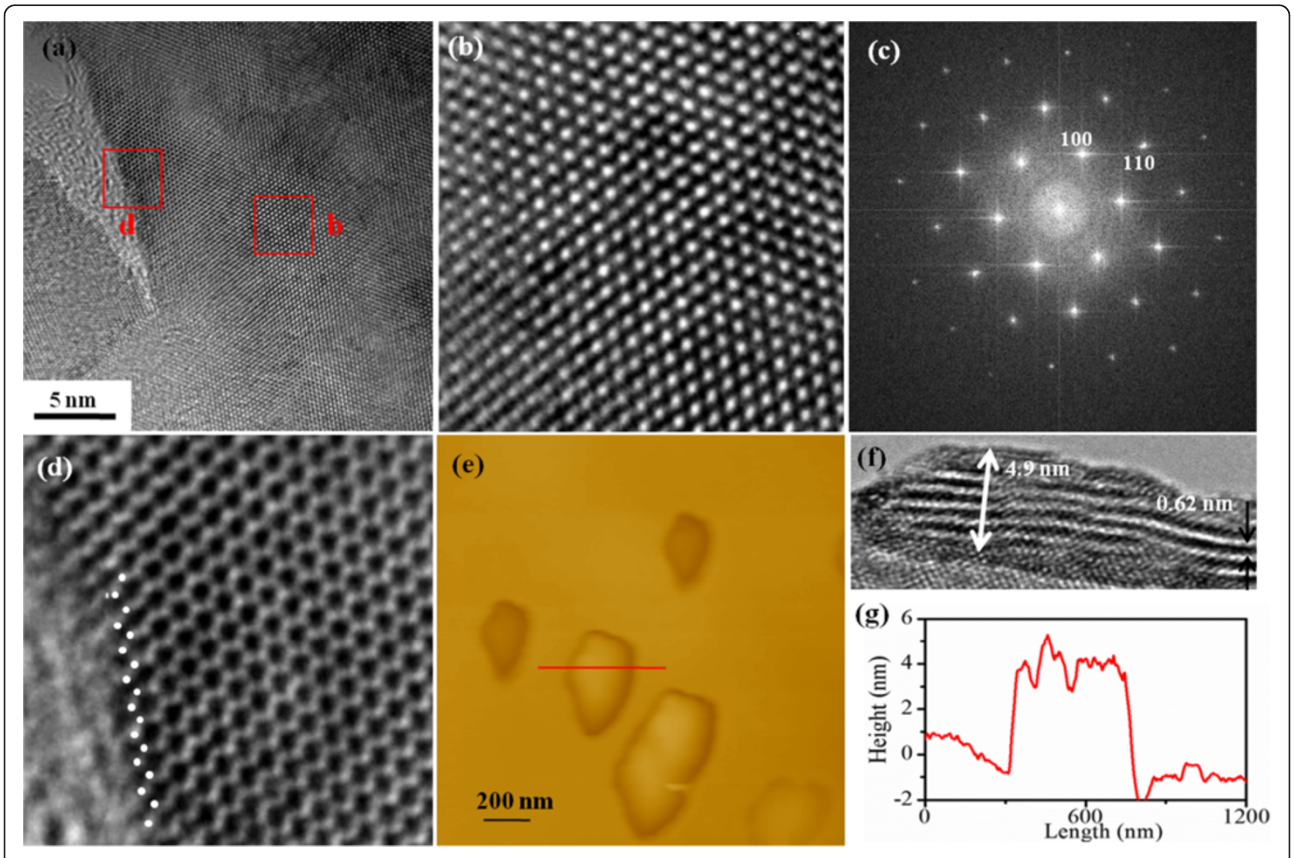


**Figure 2 Different types of imaging showing different characteristics of formed $WS_2$ nanosheets and FFT analysis. (a)** TEM image of the $WS_2$ nanosheets. **(b, d)** High-resolution TEM images for the selected regions are shown. **(c)** Two-dimensional FFT analysis for the $WS_2$ nanosheets. **(e)** Tapping-mode AFM image of the $WS_2$ nanosheets and **(g)** the corresponding thickness distribution. **(f)** High-resolution TEM image of the curled edge for the nanosheets.

density of edges. Besides, the clear bend can be observed, which may arise from defects at the edges.

The bonding characteristics and the composition of the $WS_2$ nanosheets were captured by X-ray photoelectron spectroscopy (XPS, VG ESCALAB 210; Thermo Fisher Scientific, Hudson, NH, USA), where the standard C 1*s* peak was used as a reference for correcting the shifts. Results indicate that there only W, S, and C elements are detected in the XPS survey. The peaks shown in Figure 3b, corresponding to the S $2p_{1/2}$ and S $2p_{3/2}$ orbital of divalent sulfide ions, are observed at 163.3 and 162.1 eV. Besides, the W peaks shown in Figure 3a located at 38.9, 35.5, and 33.3 eV are corresponding to W $5p_{3/2}$, W $4f_{5/2}$, and W $4f_{7/2}$, respectively. The energy positions of these peaks indicate a W valence of +4, which is in accordance with the previous reports, indicating the formation of pure $WS_2$ phase [24].

Single crystals of the bulk $WS_2$ are expected to be diamagnetic just like any other semiconductors, which is confirmed by the measured magnetization versus magnetic field (*M-H*) curve shown in Figure 4a using the Quantum Design MPMS magnetometer (Quantum Design, Inc, San Diego, CA, USA) based on superconducting quantum interference device (SQUID). However, for the $WS_2$ nanosheets, even though the magnetic response is dominated by the diamagnetism, it is found that the diamagnetic background is superimposed onto the ferromagnetic loop, implying that the total magnetic susceptibility comprises both diamagnetic and ferromagnetic parts (shown in Figure 4a). After subtracting out the diamagnetic part, the ferromagnetic response at different temperatures has been plotted in Figure 4b. The clear S-shaped saturated open curves at all the measured temperatures with the saturation magnetization ($M_s$) of 0.002 emu/g at room temperature are observed, revealing the room-temperature ferromagnetism (FM) nature of the $WS_2$ nanosheets. In addition, one can observe that the $M_s$ and the coercivity

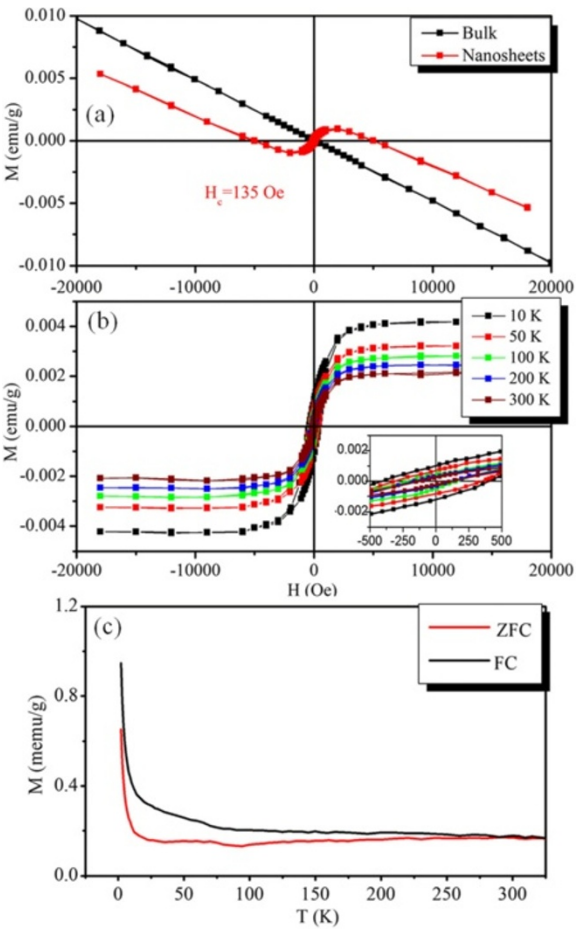


**Figure 4 M-H curves for pristine $WS_2$ bulk and nanosheets and FC and ZFC curves for $WS_2$ nanosheets. (a)** The M-H curves for the pristine $WS_2$ bulk and the $WS_2$ nanosheets. **(b)** M-H curves for the $WS_2$ nanosheets measured at different temperatures, where the diamagnetic signal has been deduced. **(c)** The FC and ZFC curves for the $WS_2$ nanosheets.

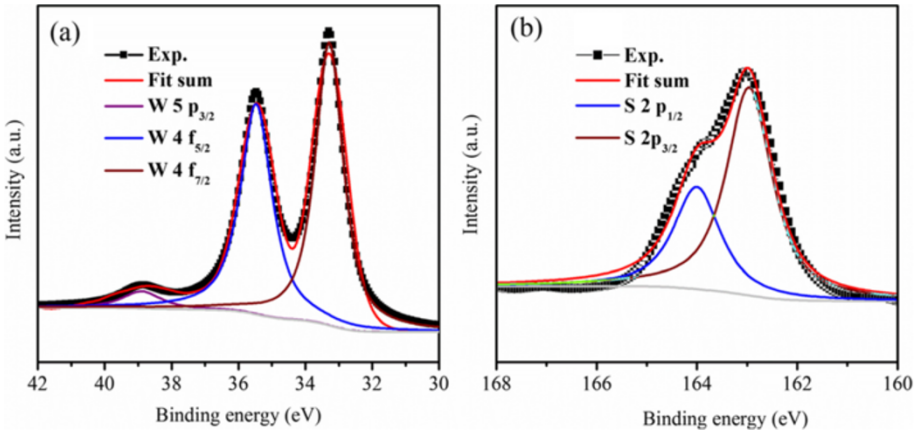


**Figure 3 High-resolution XPS scan of (a) W 5p and W 4f, (b) S 2p for $WS_2$ nanosheets.**

($H_c$) decrease as the temperature increases from 10 to 330 K, revealing a typical signature of nominal FM-like material. The temperature-dependent magnetization measurements for $WS_2$ nanosheets recorded at 100 Oe are shown in Figure 4c. The first measurement was taken after zero-field cooling (ZFC) to the lowest possible temperature (2 K), and in the second run the measurements were taken under field-cooled (FC) conditions. When cooling down from 330 K, both the ZFC and FC data follow similar trend, that is, slow increase of susceptibility until 40 K followed by a sharp rise. Note that the two curves are separated in the whole measured temperature ranges, revealing that the Curie temperature of the sample is expected to exceed 330 K.

Recently, similar ferromagnetic nature was also observed in other layered materials, like graphene, graphene nanoribbons, and $MoS_2$. Matte et al. and Enoki et al. proposed that edge states as well as adsorbed species affect the magnetic properties of graphene [25,26]. Zhang et al. prepared $MoS_2$ samples with high density of prismatic edges and showed them to be ferromagnetic at room temperature, where the magnetism arising from nonstoichiometry of the unsaturated Mo and S atoms at the edge [27]. Our previous results indicate that the saturation magnetizations of the exfoliated $MoS_2$ nanosheets increase as the lateral size decreases, revealing the edge-related ferromagnetism [22]. Density functional calculations on inorganic analog of graphite $MoS_2$ reveal that edge states are magnetic and it appears that magnetism originates at the sulfur-terminated edges due to the splitting of metallic edge states at the Fermi level [28]. Besides, calculation results indicate that only $MoS_2$-triple vacancy created in a single-layer $MoS_2$ can give rise to a net magnetic moment [29]. Shidpour et al. indicated that a vacancy on the S-edge with 50% coverage intensifies the magnetization of the edge of the $MoS_2$ nanoribbon, but such a vacancy on S-edge with 100% coverage causes this magnetic property to disappear [30]. Furthermore, $MoS_2$ and $WS_2$ clusters ($Mo_6S_{12}$ and $W_6S_{12}$) were shown to be magnetic, where the magnetism arising from the unsaturated central metal atom is due to partially filled *d* orbitals [18]. In our case, the $WS_2$ nanosheets with 2 ~ 8 layers thick and the presence of the high density of edges can be seen from the images in Figure 2f. The bends in the layers may arise from the defects. Besides, the high-resolution TEM image of the nanosheets shown in Figure 2d reveals a hexagonal arrangement of atoms with zigzag edges. Such defective centers and edges would be associated with the W atoms, which are undercoordinated, resulting in partially filled *d* orbitals. A high concentration of such edges and defects in our samples could be one of the possible reasons for the observation of ferromagnetism.

## Conclusions

In summary, even though the observed ferromagnetism in $WS_2$ is in the bulk limit, results indicate that the ferromagnetism for exfoliated $WS_2$ nanosheets persists from 10 K to room temperature. We attribute the existence of ferromagnetism partly to the zigzag edges and the defects in our samples. This unusual room-temperature ferromagnetism, which is an intrinsic feature similar to that observed in carbon-based materials, may open perspectives for spintronic devices in the future.

#### Competing interests

The authors declare that they have no competing interests.

#### Authors' contributions

DG participated in all of the measurements and data analysis, and drafted the manuscript. YX conceived and designed the manuscript. XM and QX prepared all the samples, carried out the XPS measurements and data analysis. WW participated in the SQUID measurements. All authors have been involved in revising the manuscript and read and approved the final manuscript.

#### Acknowledgements

This work is supported by the National Basic Research Program of China (grant no. 2012CB933101), NSFC (grant nos. 11034004 and 51202101), the Fundamental Research Funds for the Central Universities (no. lzujbky-2012-28), and the Specialized Research Fund for the Doctoral Program of Higher Education.

#### Author details

[1]Key Laboratory for Magnetism and Magnetic Materials of MOE, Lanzhou University, Lanzhou 730000, People's Republic of China. [2]Physics Department, Xinxiang University, Xinxiang 453003, People's Republic China.

Received: 25 June 2013 Accepted: 18 August 2013
Published: 17 October 2013

#### References

1. Aharon E, Albo A, Kalina M, Frey GL: **Growth of large-area and highly crystalline MoS2 thin layers on insulating substrates.** *Adv Funct Mater* 2006, **16:**980.
2. Lee HS, Min SW, Chang YG, Park MK, Nam T, Kim H, Kim JH, Ryu S, Im S: **MoS2 nanosheet phototransistors with thickness-modulated optical energy gap.** *Nano Lett* 2012, **12:**3695.
3. Seayad AM, Antonelli DM: **Recent advances in hydrogen storage in metal-containing inorganic nanostructures and related materials.** *Adv Mater* 2004, **16:**765.
4. Mosleh M, Atnafu ND, Belk JH, Nobles OM: **Modification of sheet metal forming fluids with dispersed nanoparticles for improved lubrication.** *Wear* 2009, **267:**1220.
5. Radisavljevic B, Radenovic A, Brivio J, Giacometti V, Kis A: **Single-layer MoS2 transistors.** *Nat Nanotech* 2011, **6:**147.
6. Mak KF, Lee C, Hone J, Shan J, Heinz TF: **Atomically thin MoS2: a new direct-gap semiconductor.** *Phys Rev Lett* 2010, **105:**136805.
7. Matte HSSR, Gomathi A, Manna AK, Late DJ, Datta R, Pati SK, Rao CNR: **MoS2 and WS2 analogues of graphene.** *Angew Chem Int Edit* 2010, **49:**4059.
8. Lauritsen JV, Kibsgaard J, Helveg S, Topsoe H, Clausen BS, Laegsgaard E, Besenbacher F: **Size-dependent structure of MoS2 nanocrystals.** *Nat Nanotech* 2007, **2:**53.
9. Zhan Y, Liu Z, Najmaei S, Ajayan PM: **Large-area vapor-phase growth and characterization of MoS2 atomic layers on a SiO2 substrate.** *Small* 2012, **8:**966.
10. Eda G, Yamaguchi H, Voiry D, Fujita T, Chen MW, Chhowalla M: **Photoluminescence from chemically exfoliated MoS2.** *Nano Lett* 2011, **11:**5111.
11. Mathew S, Gopinadhan K, Chan TK, Yu XJ, Zhan D, Cao L, Rusydi A, Breese MBH, Dhar S, Shen ZX, Venkatesan T, Thong JTL: **Magnetism in MoS2 induced by proton irradiation.** *Appl Phys Lett* 2012, **101:**102103.

12. Li H, Yin Z, He Q, Li H, Huang X, Lu G, Fam DWH, Tok AIY, Zhang Q, Zhang H: **Fabrication of single- and multilayer MoS2 film-based field-effect transistors for sensing NO at room temperature.** *Small* 2012, **8:**63.
13. Furimsky E: **Role of MoS.sub.2 and WS.sub.2 in hydrodesulfurization.** *Catal Rev Sci Eng* 1980, **22:**371.
14. Braga D, Gutiérrez Lezama I, Berger H, Morpurgo AF: **Quantitative determination of the band gap of WS2 with ambipolar ionic liquid-gated transistors.** *Nano Lett* 2012, **12:**5218.
15. Fang H, Chuang S, Chang TC, Takei K, Takahashi T, Javey A: **High-performance single layered WSe2 p-FETs with chemically doped contacts.** *Nano Lett* 2012, **12:**3788.
16. Zhao WJ, Ghorannevis Z, Chu LQ, Toh ML, Kloc C, Tan PH, Eda G: **Evolution of electronic structure in atomically thin sheets of WS2 and WSe2.** *ACS Nano* 2013, **7:**791.
17. Gutierrez HR, Perea-Lopez N, Elias AL, Berkdemir A, Wang B, Lv R, Lopez-Urias F, Crespi VH, Terrones H, Terrones M: **Extraordinary room-temperature photoluminescence in WS2 triangular monolayers.** *Nano Lett* 2013, **13:**3447.
18. Murugan P, Kumar V, Kawazoe Y, Ota N: **Atomic structures and magnetism in small MoS2 and WS2 clusters.** *Phys Rev A* 2005, **71:**063203.
19. Ma YD, Dai Y, Guo M, Niu CW, Lu JB, Huang BB: **Electronic and magnetic properties of perfect, vacancy-doped, and nonmetal adsorbed MoSe2, MoTe2 and WS2 monolayers.** *Chem Chem Phys* 2011, **13:**15546.
20. Ramakrishna Matte HSS, Maitra U, Kumar P, Rao BG, Pramoda K, Rao CNR, Anorg Z: **Synthesis, characterization, and properties of few-layer metal dichalcogenides and their nanocomposites with noble metal particles, polyaniline, and reduced graphene oxide.** *Allg Chem* 2012, **638:**2617.
21. Coleman JN, Lotya M, O'Neill A, Bergin SD, King PJ, Khan U, Young K, Gaucher A, De S, Smith RJ, Shvets IV, Arora SK, Stanton G, Kim HY, Lee K, Kim GT, Duesberg GS, Hallam T, Boland JJ, Wang JJ, Donegan JF, Grunlan JC, Moriarty G, Shmeliov A, Nicholls RJ, Perkins JM, Grieveson EM, Theuwissen K, Mccomb DW, Nellist PD, Nicolosi V: **Two-dimensional nanosheets produced by liquid exfoliation of layered materials.** *Science* 2011, **331:**568.
22. Gao DQ, Si MS, Li JY, Zhang J, Zhang ZP, Yang ZL, Xue DS: **Ferromagnetism in freestanding MoS2 nanosheets.** *Nanoscale Res Lett* 2013, **8:**129.
23. Mayer JC, Chuvilin A, Algara-Siller G, Biskupek J, Kaiser U: **Selective sputtering and atomic resolution imaging of atomically thin boron nitride membranes.** *Nano Lett* 2009, **9:**2683.
24. Yen PC, Huang YS, Tiong KK: **The growth and characterization of rhenium-doped WS2 single crystals.** *J Phys Condens Matter* 2004, **16:**2171.
25. Rao CNR, Matte HSSR, Subrahmanyam KS, Maitra U: **Unusual magnetic properties of graphene and related materials.** *Chem Sci* 2012, **3:**45.
26. Enoki T, Takai K: **Unconventional electronic and magnetic functions of nanographene-based host–guest systems.** *Dalton Trans* 2008, **8:**3773.
27. Zhang J, Soon JM, Loh KP, Yin J, Ding J, Sullivian MB, Wu P: **Magnetic molybdenum disulfide nanosheet films.** *Nano Lett* 2007, **7:**2370.
28. Vojvodic A, Hinnemann B, Nørskov JK: **Magnetic edge states in MoS2 characterized using density-functional theory.** *Phys Rev B* 2009, **80:**125416.
29. Ataca C, Sahin H, Akturk E, Ciraci S: **Mechanical and electronic properties of $MoS_2$ nanoribbons and their defects.** *J Phys Chem C* 2011, **115:**3934.
30. Shidpoura R, Manteghian M: **A density functional study of strong local magnetism creation on MoS2 nanoribbon by sulfur vacancy.** *Nanoscale* 2010, **2:**1429.

doi:10.1186/1556-276X-8-430
**Cite this article as:** Mao *et al.*: Ferromagnetism in exfoliated tungsten disulfide nanosheets. *Nanoscale Research Letters* 2013 **8**:430.